

Photophysical properties and electronic structure of retinylidene–chlorin–chalcones and analogues†

Cite this: *Photochem. Photobiol. Sci.*, 2014, **13**, 634

Joseph W. Springer,^a Masahiko Taniguchi,^b Michael Krayer,^b Christian Ruzié,^b James R. Diers,^c Dariusz M. Niedzwiedzki,^{a,d} David F. Bocian,^{*c} Jonathan S. Lindsey^{*b} and Dewey Holten^{*a}

Synthetic chlorins can accommodate diverse substituents about the macrocycle perimeter. Simple auxochromes (e.g., vinyl, acetyl, phenyl) allow systematic tuning of spectral and photophysical features. More extensive spectral tailoring may be achieved by using more potent, highly conjugated substituents that themselves bring new absorption into a target spectral region, if deleterious excited-state quenching processes can be avoided. To explore such an expanded substituent space, herein the spectral and photophysical properties of four chlorin–chalcones are reported. The molecules are free base and zinc chlorins with substituents at the 13-position that include a chalcone and an extended chalcone derived by reaction of the 13-acetylchlorin with benzaldehyde and all-*trans*-retinal, respectively. Measurements of the spectral and photophysical properties (Φ_f , τ_s , k_f , k_{IC} , k_{ISC}) are accompanied by density functional calculations that examine the characteristics of the frontier molecular orbitals. The chlorin–chalcones in nonpolar (toluene) and polar (dimethylsulfoxide) media exhibit bathochromically shifted (and intense) Q_y absorption bands. The presence of the retinylidene group adds new absorption in the blue-green region where the chlorins are typically transparent; excitation in this region leads to quantitative formation of the chlorin Q_y excited state. The spectral properties generally correlate with substituent effects on the frontier MOs. The four chlorin–chalcones in the solvent toluene have high fluorescence yields (0.24–0.30) and multi-nanosecond singlet excited-state lifetimes (3.7–8.4 ns), in addition to the added absorption imparted by the chalcone moiety. Collectively, the studies reported herein provide insight into the fundamental properties of chlorins and illustrate the utility of chalcones as a means of both tuning and augmenting the spectral properties of these chromophores.

Received 7th December 2013,
Accepted 21st January 2014

DOI: 10.1039/c3pp50421b

www.rsc.org/pps

Introduction

The utilization of tetrapyrrole macrocycles in solar light-harvesting and photomedical applications requires the ability to tailor optical and photophysical properties as well as create integrated architectures that incorporate additional constituents such as accessory pigments. The main tetrapyrrole families are porphyrins, chlorins, and bacteriochlorins, which contain zero, one or two reduced pyrrole rings, respectively. All three families of tetrapyrroles have strong absorption in the

near-UV (NUV) region, known as the Soret (or *B*) bands, corresponding to absorption from the ground electronic state (S_0) to upper (S_3 , etc.) excited states. The long-wavelength absorption band, corresponding to absorption to the lowest (S_1) excited state, is weak and in the visible region for porphyrins, stronger and in the red region for chlorins, and stronger still and in the near-infrared (NIR) region for bacteriochlorins.¹ We have previously found that the long-wavelength band of chlorins (the Q_y band) could be shifted bathochromically in ~10 nm increments from ~605 nm to ~670 nm region by placement of simple auxochromes (phenyl, vinyl, ethynyl, acetyl, formyl) at the 3- or 13-position or both.^{2–4} Analogous spectral shifts from ~710 to ~770 nm were attained upon similar attachment of such auxochromes to bacteriochlorins.^{5–7} For both families, a bathochromic shift is accompanied by intensification of the absorption band. Such spectral tuning is largely achieved by effects of the simple auxochromes on the relative energies of key frontier molecular orbitals (MOs). The MO energy shifts alter the extent of mixing of the associated excited-state electronic configurations, and thereby shift absorption intensity

^aDepartment of Chemistry, Washington University, St. Louis, Missouri 63130-4889, USA

^bDepartment of Chemistry, North Carolina State University, Raleigh, North Carolina 27695-8204, USA

^cDepartment of Chemistry, University of California, Riverside, California 92521-0403, USA. E-mail: holten@wustl.edu, jlindsey@ncsu.edu, david.bocian@ucr.edu

^dPhotosynthetic Antenna Research Center, Washington University, St. Louis, MO 63130-4889, USA

† Electronic supplementary information (ESI) available: Synthesis procedures and characterization data. See DOI: 10.1039/c3pp50421b

between the upper excited states (NUV *B* bands) and the lowest excited state (red or NIR *Q_y* band).

A potential means to elicit more profound spectral effects is to employ ‘substituents’ that inherently provide absorption in the NUV to NIR spectral region. Compared to simple auxochromes (*e.g.*, acetyl, phenyl), such entities are necessarily characterized by (1) a more extensive degree of electron delocalization (*e.g.*, extended polyene or arene), and (2) frontier MOs that are closer in energy to, and thus have the potential of mixing more substantially with, those of the tetrapyrrole (porphyrin, chlorin, bacteriochlorin) to which they are appended. As such, more potent, highly conjugated substituents may not only cause larger spectral shifts and intensity redistribution than simple auxochromes, but also introduce additional oscillator strength. The latter may include absorption in spectral regions in which a tetrapyrrole is normally transparent, thereby also serving as a tightly coupled accessory absorber. Of course, such highly conjugated species are necessarily more easily oxidized/reduced than simple auxochromes. Thus, a parallel question is the extent to which the target effects on light-harvesting capacity can be attained without compromising desirable photophysical properties such as long excited-state lifetimes.

To examine such possibilities, we recently explored the use of ‘chalcone’ (*i.e.*, enone) substituents at the 3- and 13-positions of bacteriochlorins and extended the absorption even further into the NIR region, again with an increase in intensity.⁸ One significant attraction of chalcones is the ease of formation. Of equal importance is the absorption provided by the chalcone moiety itself, which can be tailored by the length of the polyene unit and the nature of the terminal groups. Indeed, the term chalcone was first used at the end of the 19th century to denote the characteristic copper-like color of the enone condensation product of benzaldehyde and acetophenone.⁹ The literature on chalcones (*i.e.*, α,β -enones) is now vast⁸ owing to preparation of diverse synthetic products^{10,11} and recognition that the chalcone substructure appears in a wide variety of natural products.^{12–15}

Herein, we use static and time-resolved optical spectroscopy to examine the absorption spectra and other photophysical properties of synthetic chlorins that contain chalcone substituents. The chlorin–chalcones explored are shown in Chart 1 and include the free base (Fb) form and zinc (Zn) chelate of the chlorin (C). Each chlorin–chalcone contains a 10-mesityl group, which is present in 13-acetyl benchmarks **ZnC-A** and **FbC-A** but not in the unsubstituted parent chlorins **ZnC** and **FbC**. The retinylidene–chlorin–chalcones (**FbC-6**, **ZnC-6**) are examples of two commonplace chromophores joined *via* a readily constructed linker. Two additional chlorin–chalcones (**FbC-1**, **ZnC-1**) contain the shortest chalcone possible. Benchmark chalcone **I** that contains six carbon–carbon double bonds was also prepared by reaction of all-*trans*-retinal and acetophenone (Chart 1).

Analysis of the photophysical properties is aided by molecular-orbital (MO) characteristics obtained from density-functional theory (DFT) calculations. Key findings are (1) a chalcone

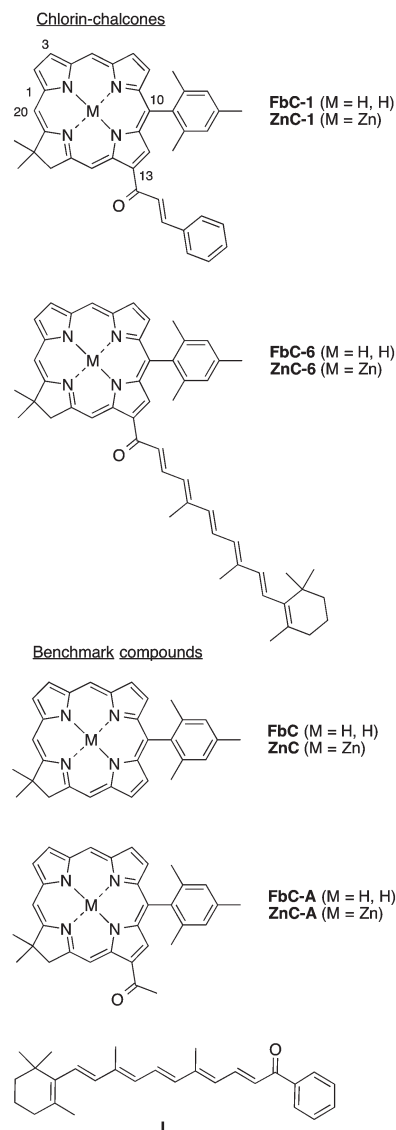


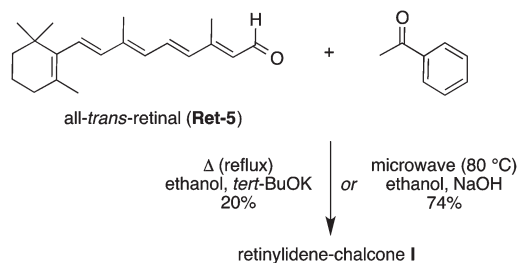
Chart 1 Chlorin–chalcones (top) and benchmark compounds (bottom).

tightly coupled to a chlorin introduces new absorption in the blue-green region (to upper excited states of the combined construct), (2) the presence of the chalcone does not substantially alter the photophysical properties of the chlorin singlet excited state except in a few cases (depending on chalcone and solvent polarity), and (3) the effects of chalcone *versus* simple auxochromic substituents can be generally rationalized by correlating with the energies and electron-density distributions of the frontier MOs. Collectively, the study has produced chlorins with enhanced absorption and favorable excited-state properties for utility in light-harvesting systems.

Results

Synthesis

The chlorin–chalcones described herein were prepared previously¹⁶ with the exception of **ZnC-6**. The zinc chlorin **ZnC-6**



Scheme 1 Synthesis of benchmark retinylidene-chalcone I.

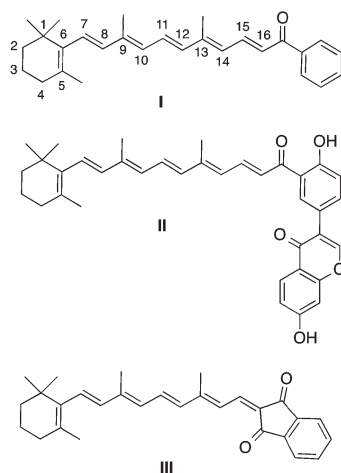


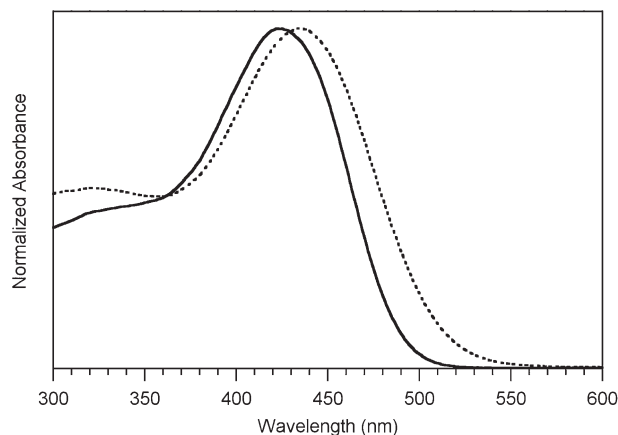
Chart 2 Retinylidene-chalcones.

was obtained by zincation¹⁷ of the free base chlorin **FbC-6**. The benchmark chlorins **ZnC**,¹⁸ **FbC**,¹⁹ **ZnC-A**¹⁸ were prepared as described previously. The known benchmark chlorin **FbC-A**¹⁶ was prepared here by demetalation of the zinc chelate **ZnC-A**. The benchmark chalcone (**I**) was obtained as a red oil upon reaction of acetophenone and all-*trans*-retinal (Scheme 1). The reaction with microwave irradiation afforded a substantially higher yield *versus* traditional heating.

The structure of **I** can be compared with those of other known retinylidene-chalcones **II** and **III** (Chart 2). The absorption spectrum of **I** in toluene and in dimethylsulfoxide (DMSO) at room temperature is shown in Fig. 1. The main absorption band of compound **I** ($\epsilon_{423 \text{ nm}} = 37\,400 \text{ M}^{-1} \text{ cm}^{-1}$ in toluene) can be compared with values for **II** ($\epsilon_{442 \text{ nm}} = 44\,600 \text{ M}^{-1} \text{ cm}^{-1}$ in methanol)²⁰ or **III** ($\epsilon_{484 \text{ nm}} = 65\,000 \text{ M}^{-1} \text{ cm}^{-1}$ in *n*-hexane;²¹ $\epsilon_{490 \text{ nm}} = 49\,800 \text{ M}^{-1} \text{ cm}^{-1}$ in ethanol²²). The ¹H NMR spectra of retinals have been thoroughly examined and complete assignments are available.^{21,23} The ¹H NMR spectrum of **I** has been examined by H-H COSY and NOESY protocols. The assignments are listed in Table 1 together with those for two other retinylidene-chalcones (**II**, **III**) and for all-*trans*-retinal.

Photophysical characterization of chlorins

Absorption spectra. Fig. 2A shows the absorption spectrum of the zinc chelates of the parent chlorin (**ZnC**), the

Fig. 1 Absorption spectra of the retinylidene-chalcone **I** in toluene (solid) and DMSO (dashed) normalized at the local maxima (423, 434 nm).Table 1 ¹H NMR chemical shifts (δ , ppm) of retinylidene-chalcones

Proton positions	All- <i>trans</i> -retinal ^a	I ^b	II ^c	III ^d
1- <i>gem</i> -CH ₃	1.03	1.04	1.03	1.13
2-CH ₂ -	1.47	1.47	1.45	1.48
3-CH ₂ -	1.62	1.61	1.58	1.59
4-CH ₂ -	2.03	2.02	2.14	1.97
5-CH ₃	1.72	1.73	1.70	1.79
9-CH ₃	2.03	2.01	2.01	1.77
13-CH ₃	2.32	2.13	2.09	1.67
7-H	6.33	6.27	6.30	6.39
8-H	6.16	6.16	6.19	6.31
10-H	6.18	6.18	6.25	6.04
11-H	7.14	6.89	7.04	6.82
12-H	6.37	6.41	6.58	6.31
14-H	5.97	6.38	6.51	8.32
15-H	10.10	7.91	7.90	8.05
16-H	—	7.01	7.48	—

^aThe chemical shifts are from ref. 24; assignments are from ref. 20; all in CDCl₃. ^bThis work, in CDCl₃. ^cRef. 20, in DMSO-*d*₆. ^dRef. 21, in benzene-*d*₆.

13-acetylchlorin benchmark (**ZnC-A**), and the 13-chalcone-chlorins (**ZnC-1** and **ZnC-6**) in toluene. Spectra for the same four compounds in DMSO are given in Fig. 2B. Spectra for the free base analogues are presented in Fig. 2C and 2D. Each spectrum contains the basic elements expected for a chlorin, plus additional blue-region absorption for **ZnC-6** and **FbC-6**. Progressing from longer to shorter wavelengths, the main tetrapyrrole features (and rough spectral ranges) are Q_y (590–690 nm), Q_x (470–560 nm), B_x (390–430 nm), and B_y (390–430 nm). Each origin band is typically accompanied by a weaker vibronic overtone feature 1000–1500 cm⁻¹ at shorter wavelength. The weak Q_x bands (origin and overtone) are more apparent for the free base chlorins than the zinc chelates. The nominal B_x and B_y (Soret) features are coalesced for **ZnC** and **ZnC-A** and become separated by varying degrees for **ZnC-1** and **ZnC-6** and the free base analogues.

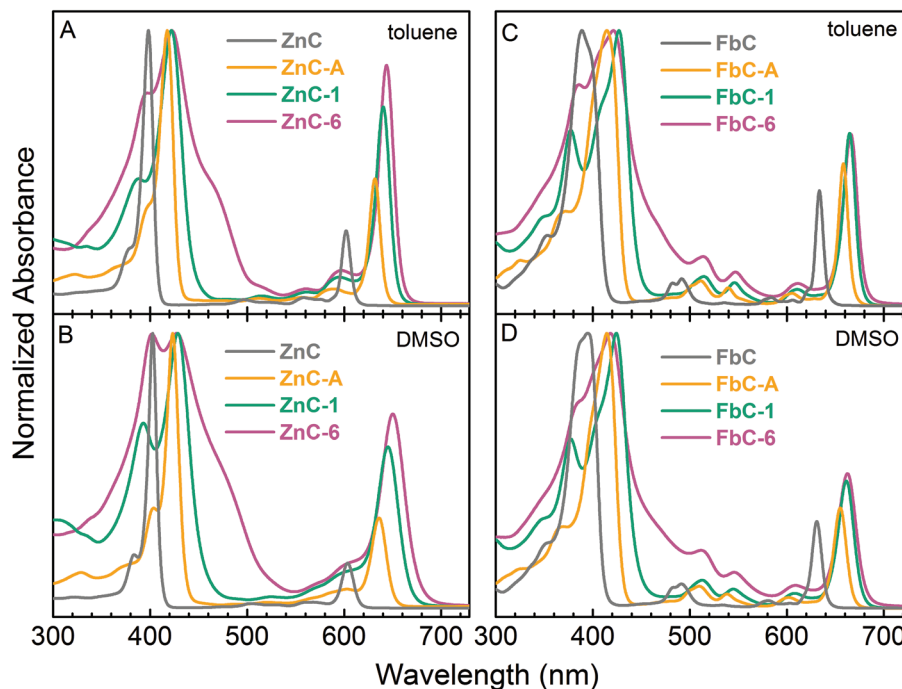


Fig. 2 Absorption spectra of the zinc chlorins (A, toluene; B, DMSO) and free base chlorins (C, toluene; D, DMSO) normalized at the maximum in the Soret region.

The spectra in Fig. 2 are normalized at the Soret (B) maximum, which is a common manner of presenting spectra for photosynthetic chromophores and analogues to help visualize variations in the peak intensity of the Q_y band. Such normalization does not always provide a quantitative assessment, because substituents may alter the overlap of the B_x and B_y components as well as the relative bandwidths of these features and the Q_y band. [Plots on the basis of molar absorption (extinction) coefficients are also often misleading due to significant measurement errors.] To roughly capture variations in the Soret manifold, Fig. 3 presents the spectra normalized to the integrated absorption in the 350–450 nm region. This range encompasses the main Soret absorption while rejecting most of the additional absorption (>450 nm) associated with the presence of the 13-retinylidene group of **ZnC-6** and **FbC-6**. This normalization method also has shortcomings (such as not accounting for changes in Q_y bandwidth), but provides a more faithful first-order visualization of the variation in Q_y peak intensity among compounds. The 450 nm cutoff used to construct Fig. 3 is arbitrary, and this presentation is not meant to imply that the 13-retinylidene group and chlorin macrocycle can be considered independent entities, which they are almost certainly not (*vide infra*). Values for the peak position, full-width-at-half-maximum (FWHM), Q_y/B peak-intensity ratio (I_{Q_y}/I_B) and Q_y/B integrated-intensity ratio (Σ_{Q_y}/Σ_B) are collected in Table 2.

Previous studies have shown that the 15–20 nm bathochromic shift and intensification of the Q_y band for the 10,13-substituted **ZnC-A** and **FbC-A** versus parent chlorins **ZnC** and **FbC** derive primarily from the 13-acetyl group.^{2,3} The intensification of Q_y is relative to the Soret and is indicated by both I_{Q_y}/I_B and

Σ_{Q_y}/Σ_B (Table 2), the latter taking into account the Q_y bandwidth, which is not included in the normalization used in Fig. 3. A 10-mesityl (or phenyl or *p*-tolyl) group (not present in **ZnC** or **FbC**) causes a bathochromic shift of only 3–5 nm and instead a small diminution of Q_y intensity.^{3,4,17} Replacement of the 13-acetyl group with the short chalcone group of **ZnC-1** and **FbC-1** gives rise to an additional bathochromic shift and intensification of the Q_y band, albeit generally not as substantial as the addition of the acetyl group to a parent chlorin. There is a somewhat larger (relative to the short chalcone) bathochromic shift upon replacement with the longer chalcone group of **ZnC-6** and **FbC-6**. Consideration of the Σ_{Q_y}/Σ_B values in Table 2 (and associated errors) indicates that potential intensification of the Q_y band for the chalcone groups containing six versus one carbon–carbon double bond(s) may depend on the metalation state (zinc versus free base) and/or solvent (toluene versus DMSO).

The Soret (B) maximum also shifts bathochromically along the series **ZnC** < **ZnC-A** < **ZnC-1** < **ZnC-6** and the series **FbC** < **FbC-A** < **FbC-1** < **FbC-6** (Fig. 2). The shift upon incorporation of a 13-acetyl group and then chalcone moieties bearing one or six carbon–carbon double bonds likely reflects an increase in splitting of the B_y and B_x components as well as an increase in breadth of these features. The most substantial effects on the Soret contour are observed for the chlorin–chalcones that contain the retinylidene unit, and are greater for **ZnC-6** than **FbC-6**. The broadening of the Soret contour for the latter two compounds (in both toluene and DMSO) likely derives from the above-noted effects plus additional absorption in the 450–500 nm region due to the presence of the long chalcone

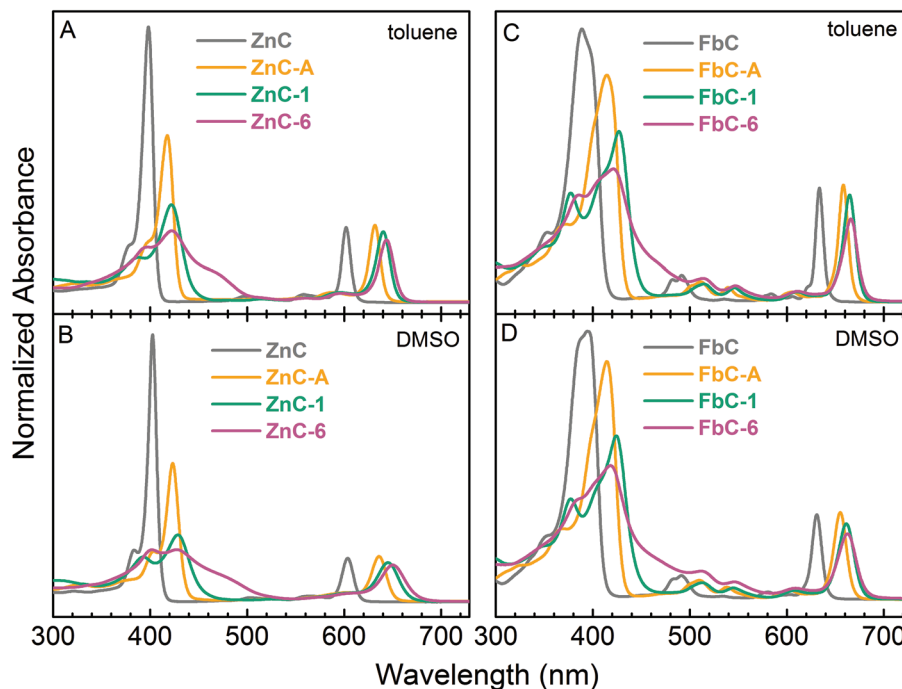


Fig. 3 Absorption spectra of the zinc chlorins (A, toluene; B, DMSO) and free base chlorins (C, toluene; D, DMSO) normalized by the integrated absorption in the 350–450 nm (Soret) region.

Table 2 Spectral properties of chlorin–chalcones and benchmarks^a

Compound	Solvent	B_{\max} abs (nm)	Q_y abs (nm)	Q_y abs FWHM (nm)	$I_{Q_y}/I_{B_{\max}}$	Σ_{Q_y}/Σ_B	Q_y flu (nm)	Q_y flu FWHM (nm)
ZnC	Toluene	398	602	11	0.28	0.23	604	12
ZnC-A	Toluene	418	631	14	0.45	0.32	635	15
ZnC-1	Toluene	422	640	17	0.69	0.37	646	18
ZnC-6	Toluene	423	644	20	0.89	0.36	648	23
FbC	Toluene	389	633	10	0.42	0.17	635	12
FbC-A	Toluene	414	658	12	0.52	0.21	661	14
FbC-1	Toluene	426	665	15	0.62	0.26	669	16
FbC-6	Toluene	421	666	17	0.62	0.25	670	18
ZnC	DMSO	403	604	14	0.16	0.17	608	15
ZnC-A	DMSO	423	636	19	0.32	0.34	642	20
ZnC-1	DMSO	429	645	28	0.59	0.45	650	31
ZnC-6	DMSO	402/427 ^b	650	31	0.72	0.45	658	33
FbC	DMSO	395	631	12	0.31	0.12	633	14
FbC-A	DMSO	414	655	15	0.36	0.21	660	17
FbC-1	DMSO	424	661	20	0.46	0.25	668	21
FbC-6	DMSO	418	663	24	0.49	0.31	665	25

^a All absorption (abs) and fluorescence (flu) data were obtained at room temperature. ^b The two Soret features have approximately equal intensity.

substituent. Broad absorption in this blue-green region is exhibited by the long-chalcone benchmark I (Fig. 1).

Subtle changes in spectral properties of the chlorins (chalcone-substituted and benchmarks) are observed as the solvent is changed from toluene to DMSO (Fig. 2 and 3 and Table 2). The switch to the more polar solvent gives a bathochromic shift in the Soret (B) maximum (4–7 nm), a bathochromic shift in the Q_y maximum for the zinc chelates (2–6 nm), a hypsochromic shift in the Q_y band for the free base chlorins (2–4 nm), and a broadening of the Q_y band for all compounds (20–65%). The greater Q_y FWHM for the compounds in DMSO

versus toluene is paralleled by a decrease in relative Q_y/B peak-intensity ratio (I_{Q_y}/I_B) and is taken into account in the integrated-intensity ratio (Σ_{Q_y}/Σ_B).

Fluorescence spectra. The fluorescence spectra for the chlorin–chalcones and corresponding benchmarks are dominated by the Q_y origin band (Fig. 4). The spectra are typical of previously studied chlorins.^{2,4,17} The Q_y fluorescence maximum for each zinc chlorin is bathochromically shifted 2–8 nm in DMSO *versus* toluene, paralleling the solvent effect on the Q_y absorption maximum (Table 2). The opposite effect is seen for the free base chlorins, with a 1–5 nm hypsochromic

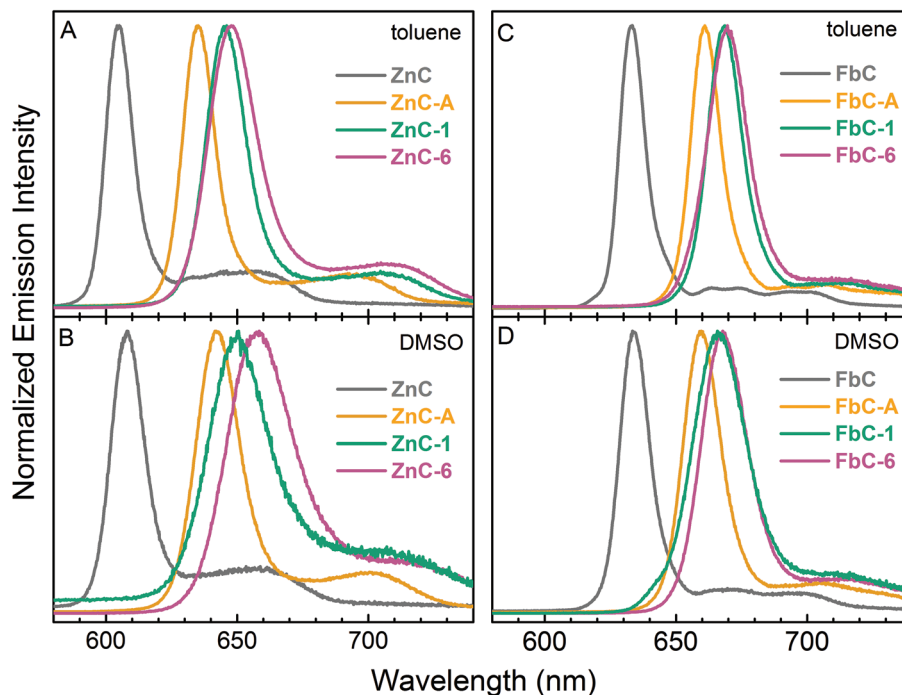


Fig. 4 Normalized fluorescence spectra of zinc chlorins (A, toluene; B, DMSO) and free base chlorins (C, toluene; D, DMSO).

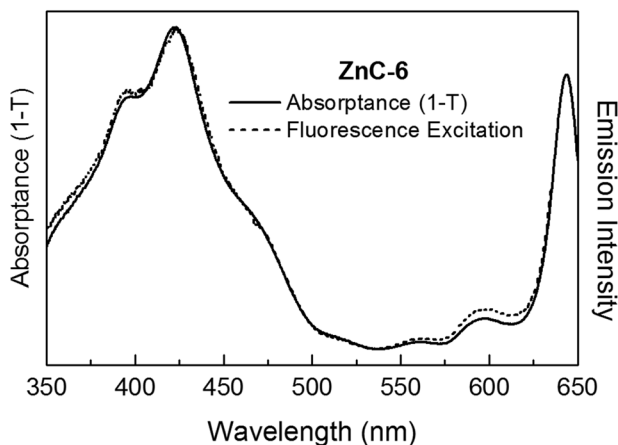


Fig. 5 Normalized absorbance ($1 - T$) spectrum and fluorescence-excitation spectrum ($\lambda_{em} = 650$ nm) for **ZnC-6** in toluene.

shift in DMSO compared to toluene, also consistent with the Q_y absorption shift. Both the zinc and free base chlorins exhibit broader emission peaks in DMSO *versus* toluene, with the largest change observed for the zinc chlorin–chalcones (10–13 nm FWHM increase; Table 2).

A pertinent question is whether the new absorption in the 450–500 nm region for **ZnC-6** and **FbC-6**, which is not observed for typical chlorins such as **ZnC-A** and **FbC-A** (Fig. 2 and 3), leads to chlorin Q_y fluorescence. This issue is addressed in Fig. 5, which compares the absorbance [$= 1 - \text{transmittance}$ (T)] spectrum of **ZnC-6** with the excitation spectrum of the fluorescence ($\lambda_{det} = 650$ nm) from this compound. Both spectra are for the compounds in toluene and are normalized

at the Soret maximum. The excellent match of the two spectra, including in the 450–500 nm region, indicates that the new absorption due to the retinylidene group in **ZnC-6** and **FbC-6** leads to the quantitative formation of the Q_y excited state. Similar results are obtained for **FbC-6** in toluene and both compounds in DMSO, albeit with differences in inherent fluorescence yield due to differences in the decay properties of the Q_y excited state (*vide infra*).

Excited-state properties. The lowest-energy singlet excited state (S_1) of each chlorin–chalcone and chlorin benchmark decays by $S_1 \rightarrow S_0$ spontaneous fluorescence, $S_1 \rightarrow S_0$ internal conversion, and $S_1 \rightarrow T_1$ intersystem crossing with respective rate constant k_f , k_{ic} or k_{isc} ; yield Φ_f , Φ_{ic} or Φ_{isc} ; and lifetime $\tau_S = (k_f + k_{ic} + k_{isc})^{-1}$. Table 3 lists the measured values of τ_S , Φ_f and Φ_{isc} and the value of Φ_{ic} calculated from the formula $\Phi_{ic} = 1 - \Phi_f - \Phi_{isc}$. The table also gives the three rate constants, obtained using the expression $k_i = \Phi_i/\tau_S$ (with $i = f, ic, isc$).

The chlorin–chalcones (**ZnC-1**, **ZnC-6**, **FbC-1**, **FbC-6**) in toluene exhibit fluorescence yields (0.24–0.30) that are generally greater than those for the benchmarks (**ZnC-A**, **FbC-A**) and all the synthetic chlorins that we have studied,^{2–4} approaching that of the native chlorophyll *a* (0.325).^{25,26} The large Φ_f values reflect the increased k_f values (because $\Phi_f = \tau_S k_f$), which in turn are related *via* the Einstein coefficients²⁷ to the above-noted Q_y ($S_0 \rightarrow S_1$) absorption. The k_f (and Φ_f) values and Q_y absorption strength (as indicated by Σ_{Q_y}/Σ_B) increase in the order **ZnC** < **ZnC-A** < **ZnC-1** and **FbC** < **FbC-A** < **FbC-1** for the compounds in toluene and DMSO (Tables 2 and 3). The k_f value for **FbC-6** is comparable to that for **FbC-1**, while that for **ZnC-6** cannot be obtained because the τ_S value is not due to the (pure) S_1 state (*vide infra*). Overall, the good correlation of

Table 3 Excited-state properties of chlorin–chalcones and benchmarks^a

Compound	Solvent	τ_S (ns)	Φ_f	Φ_{isc}	Φ_{ic}	k_f^{-1} (ns)	k_{isc}^{-1} (ns)	k_{ic}^{-1} (ns)
ZnC	Toluene	1.7	0.06	0.88	0.06	27	2	29
ZnC-A	Toluene	4.7	0.24	0.64	0.12	20	7	39
ZnC-1	Toluene	4.6	0.26	0.64	0.10	18	7	45
ZnC-6	Toluene	3.7	0.28	0.47	0.25	13	8	15
FbC	Toluene	8.8	0.20	0.61	0.19	44	14	46
FbC-A	Toluene	9.9	0.26	0.52	0.22	38	19	45
FbC-1	Toluene	8.4	0.30	0.41	0.29	28	20	29
FbC-6	Toluene	7.2	0.24	0.39	0.37	30	18	19
ZnC	DMSO	1.8	0.070	0.80	0.06	27	2	29
ZnC-A	DMSO	5.6	0.25	^b		22		
ZnC-1	DMSO	3.2	0.15	0.40	0.45	21	8	7
ZnC-6	DMSO	0.015 ^c	0.006	≤ 0.01				
FbC	DMSO	9.3	0.17	0.67	0.19	44	14	46
FbC-A	DMSO	9.3	0.24	0.61	0.22	38	19	45
FbC-1	DMSO	7.3	0.24	0.51	0.29	28	20	29
FbC-6	DMSO	1.0/7.4 ^d	0.13	0.48	0.39	32	11	9

^a All measurements were made at room temperature. The errors in the measured quantities are as follows: $\tau_S \pm 5\%$, $\Phi_f \pm 10\%$, $\Phi_{isc} \pm 10\%$. ^b The apparent Φ_{isc} (0.79) is too high to allow reliable estimation of rate constants. ^c The decay measured transient absorption has a dominant 15 ps component and a minor ($\sim 5\%$) 0.4 ns phase. Rate constants are not calculated because the chlorin τ_S may be shorter than 15 ps, which instead would reflect the decay of a lower energy state fed by the chlorin S_1 (Q_y) state. ^d Two decay components with equal amplitudes. The rate constants are averages based on the two lifetime components.

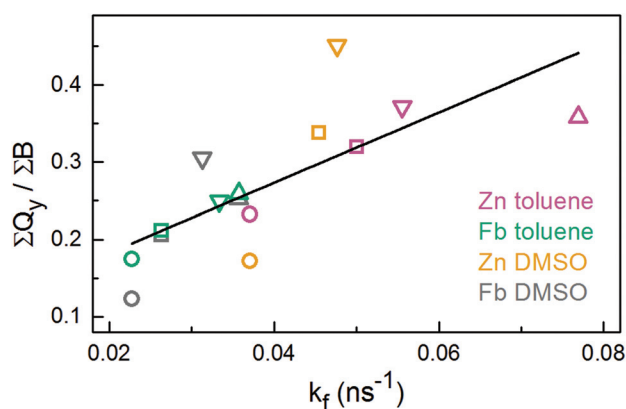


Fig. 6 Intensity ratio of the *B* and Q_y absorption manifolds versus the radiative rate constant determined from the fluorescence yield and single excited-state lifetime. Data for the four zinc (Zn) chelates and free base (Fb) analogues in toluene and DMSO are color coded as indicated. The symbols further identify the compounds as follows: ZnC and FbC (circles), ZnC-A and FbC-A (squares), ZnC-1 and FbC-1 (down triangles), and ZnC-6 and FbC-6 (up triangles).

the k_f and $\Sigma Q_y/\Sigma B$ values shown in Fig. 6 reflects consistency of the various measurements and analysis.

One of two exceptions to the above-noted trends is **FbC-6** in DMSO, for which Φ_f (0.13) is about half that for **FbC-1** in DMSO (0.24), and the excited-state decay has τ_S components of ~ 1 ns and ~ 7.4 ns with roughly equal amplitudes. The longer τ_S component is similar to that for **FbC-1** in DMSO. Nonetheless, the k_f of $(32 \text{ ns})^{-1}$, calculated from Φ_f and the amplitude-weighted τ_S , is comparable to the value of $(28 \text{ ns})^{-1}$ for **FbC-1** and correlates with the relative Q_y intensity (Fig. 6). The reduced Φ_f and short τ_S component reflect enhanced $S_1 \rightarrow S_0$

internal conversion (k_{ic} , Table 3) in one of two (or more) excited-state populations (*vide infra*).

The most significant exception to the trends in photo-physical properties is found for **ZnC-6** in DMSO, where internal conversion is so enhanced that, despite an expected increased k_f (based on $\Sigma Q_y/\Sigma B$), Φ_f is reduced to 0.006 and τ_S to ~ 15 ps or less (Table 3). Fig. 7 shows representative transient absorption data for **ZnC-6** in DMSO, revealing the ultrafast excited-state decay and (complete) ground-state recovery compared to the multi-nanosecond excited-state decay (and high yield of the long-lived T_1 excited state) for the compound in toluene. Furthermore, the broad absorption between 500 and 630 nm (Fig. 7B) versus the relatively featureless absorption in toluene (Fig. 7A) suggests some difference in character of the excited state observed in the two media. Such a difference in spectra is suggestive of charge-transfer (CT) character. However, the amount of CT character is not clear because analogous spectral differences are observed for **ZnC-1** and **ZnC-A** in DMSO versus toluene, but not for **ZnC**.

Photophysical properties of retinylidene benchmark I

The benchmark for the chalcone substituent with six carbon-carbon double bonds (**I**) is essentially non-fluorescent in both toluene and DMSO. Thus, the excited-state decay properties were studied using ultrafast transient absorption spectroscopy. The transient absorption spectra are generally similar for **I** in the two media (Fig. 8). The spectra display broad (positive) absorption from 500 to 700 nm, with the expected (negative) ground-state bleaching feature dominating at shorter wavelengths. Global fits of the time profiles across the spectral region probed return lifetimes of 6.5 ps and 60 ps (1 : 1 ratio) in toluene, and 15 ps in DMSO (Fig. 8C).

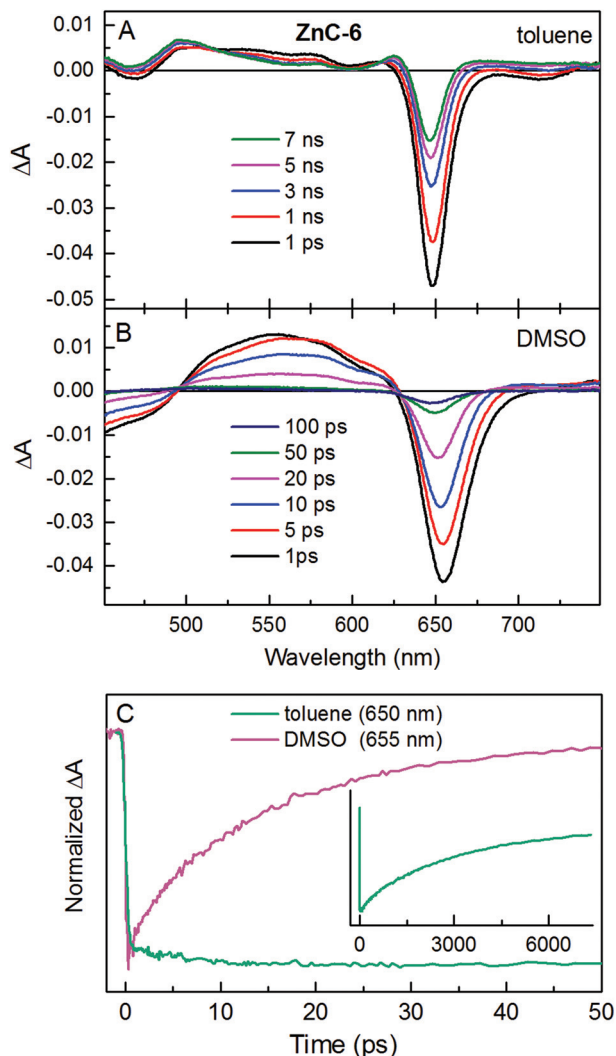


Fig. 7 Transient absorption spectra for ZnC-6 in toluene (A) and DMSO (B), and representative kinetic traces at 633 nm (C), obtained using excitation with ~ 100 fs flashes at ~ 420 nm.

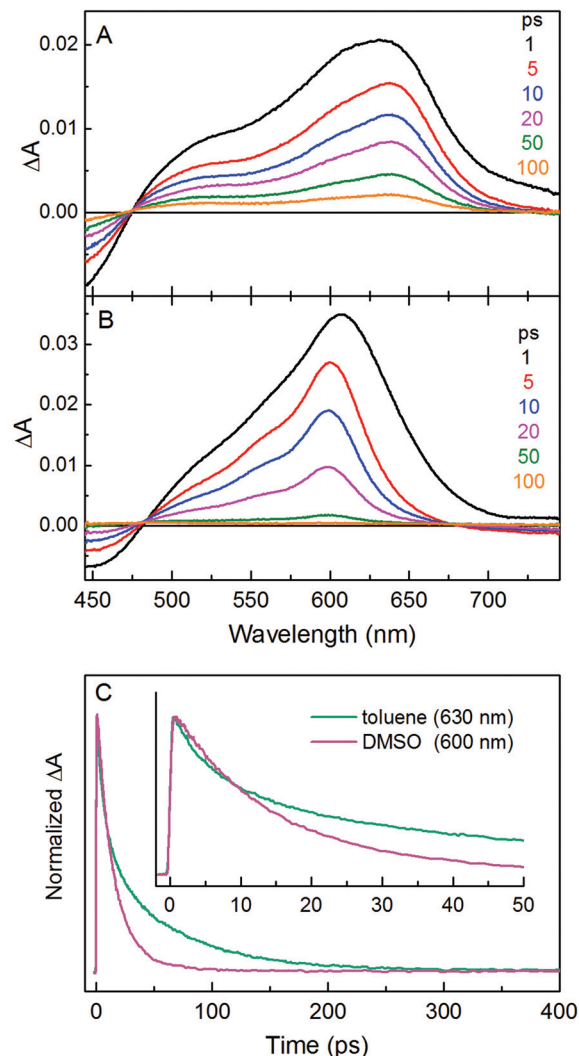


Fig. 8 Transient absorption spectra for I in toluene (A) and DMSO (B), and time profiles (C), obtained using ~ 100 fs excitation flashes at 420 nm.

Molecular-orbital characteristics

The MO characteristics were obtained from DFT calculations. Fig. 9 shows the electron-density distributions and energies for the highest occupied MO (HOMO), the lowest unoccupied MO (LUMO) as well as the HOMO-1 and LUMO+1 for the zinc chlorin-chalcones and chlorin benchmarks. Fig. 10 shows results for the free base analogues. The lettered arrows in Fig. 9 and 10 indicate correlation of an orbital or boxed pair of orbitals with one of the four “normal” chlorin frontier MOs (HOMO-1, HOMO, LUMO, LUMO+1 of ZnC or FbC) as the 13-substituent is changed from none to acetyl to short chalcone (one carbon-carbon double bond) to long chalcone (retinylidene; six carbon-carbon double bonds). Fig. 11 shows MO characteristics for I, which also serves as a benchmark for the long 13-chalcone substituent of ZnC-6 and FbC-6. Fig. 11 also shows the MO properties for a benchmark for the 13-acetyl group of ZnC-A and FbC-A (acetophenone) and for

the shorter 13-chalcone group of ZnC-1 and FbC-1 (benzylideneacetophenone, denoted IV). MO energies and the LUMO-HOMO energy gap for all the molecules are listed in Table 4.

Discussion

The ability to tailor the spectral and photophysical properties of hydroporphyrins is of fundamental interest for capturing red and NIR light. The ability to integrate such hydroporphyrins with other constituents and in larger architectures is essential to meet the needs for diverse applications. The use of the chalcone substituent may satisfy both objectives in affording a bathochromic shift of the Q_y absorption band and, most importantly, imparting absorption in a region where the chlorin absorbs little if at all. Indeed, the chlorin-chalcones

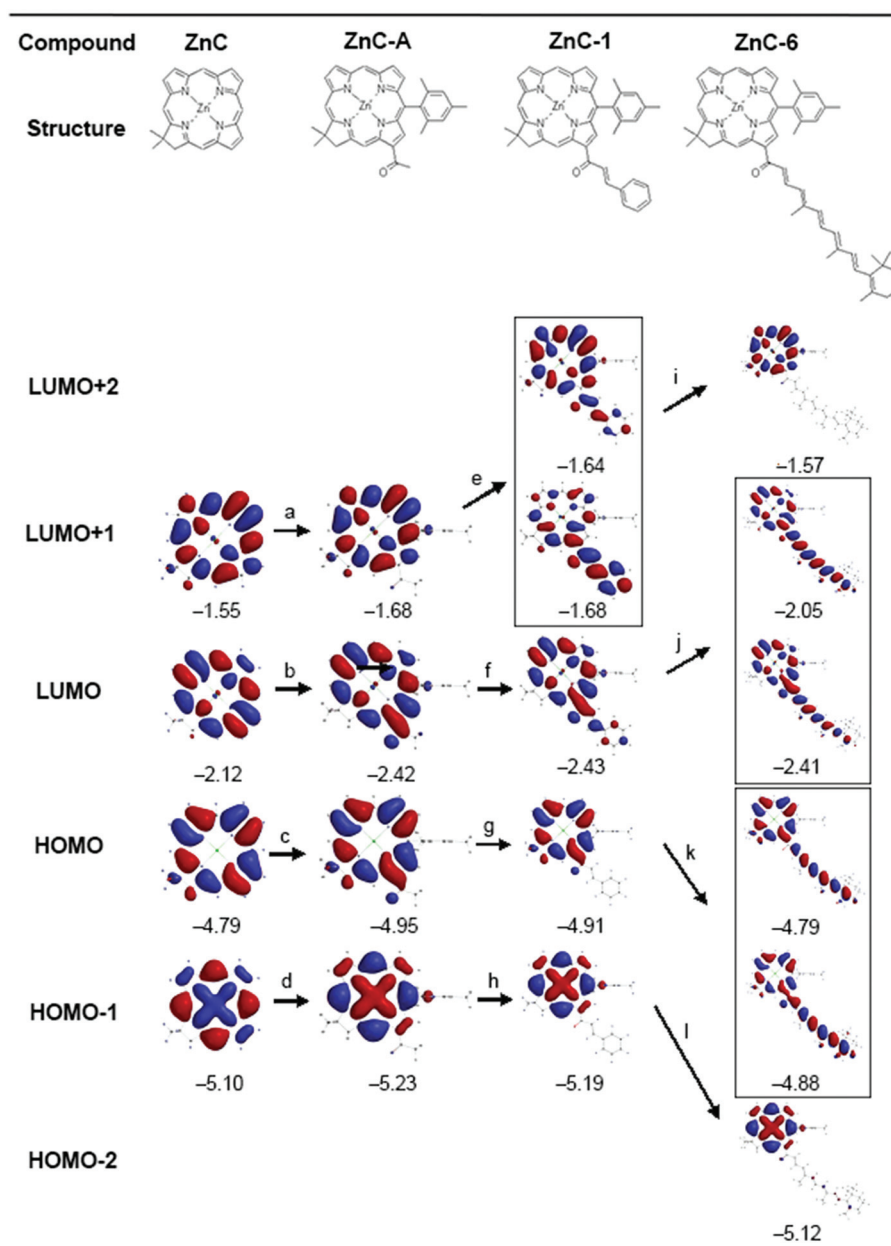


Fig. 9 Characteristics of the three lowest unoccupied and three highest occupied MOs of zinc chlorins. The lettered arrows indicate correlation of an orbital or boxed pair of orbitals with one of the four "normal" chlorin frontier MOs (HOMO–1, HOMO, LUMO, LUMO+1 of ZnC) as the 13-substituent is changed from none to acetyl to short chalcone to long chalcone.

(ZnC-1, FbC-1, ZnC-6, FbC-6) in nonpolar (toluene) and polar (DMSO) media exhibit bathochromically shifted (and intense) Q_y absorption bands *versus* that of most other synthetic chlorins.^{2,3} Furthermore, the presence of the retinylidene group in ZnC-6 and FbC-6 adds new absorption in the 450–500 nm region where chlorins are typically transparent. This new absorption increases the integrated (350–750 nm) absorption capacity by 10–15% (compared to benchmarks that lack a chalcone substituent) and leads to quantitative formation (*via* internal conversion) to the chlorin Q_y excited state of ZnC-6 and FbC-6. Moreover, the four chlorin–chalcones in toluene have high fluorescence yields and multi-nanosecond singlet

excited-state lifetimes (3.7–8.4 ns) that can support efficient excited-state energy or charge transfer depending on the application. Even in DMSO the Φ_f and τ_S values of ZnC-1 (0.15, 3.2 ns), FbC-1 (0.24, 7.3 ns) and FbC-6 (0.13, 1.0/7.4 ns) are substantial. Only for ZnC-6 (and the short τ_S component for FbC-1) in DMSO does the presence of the (long) chalcone group result in significant quenching of the chlorin Q_y excited state (0.006, ≤ 15 ps). We now turn to exploring how these properties derive from the composition and electronic structure of the architectures.

In the following subsections, we begin with an overview of molecular design, which is followed by a brief comparison of

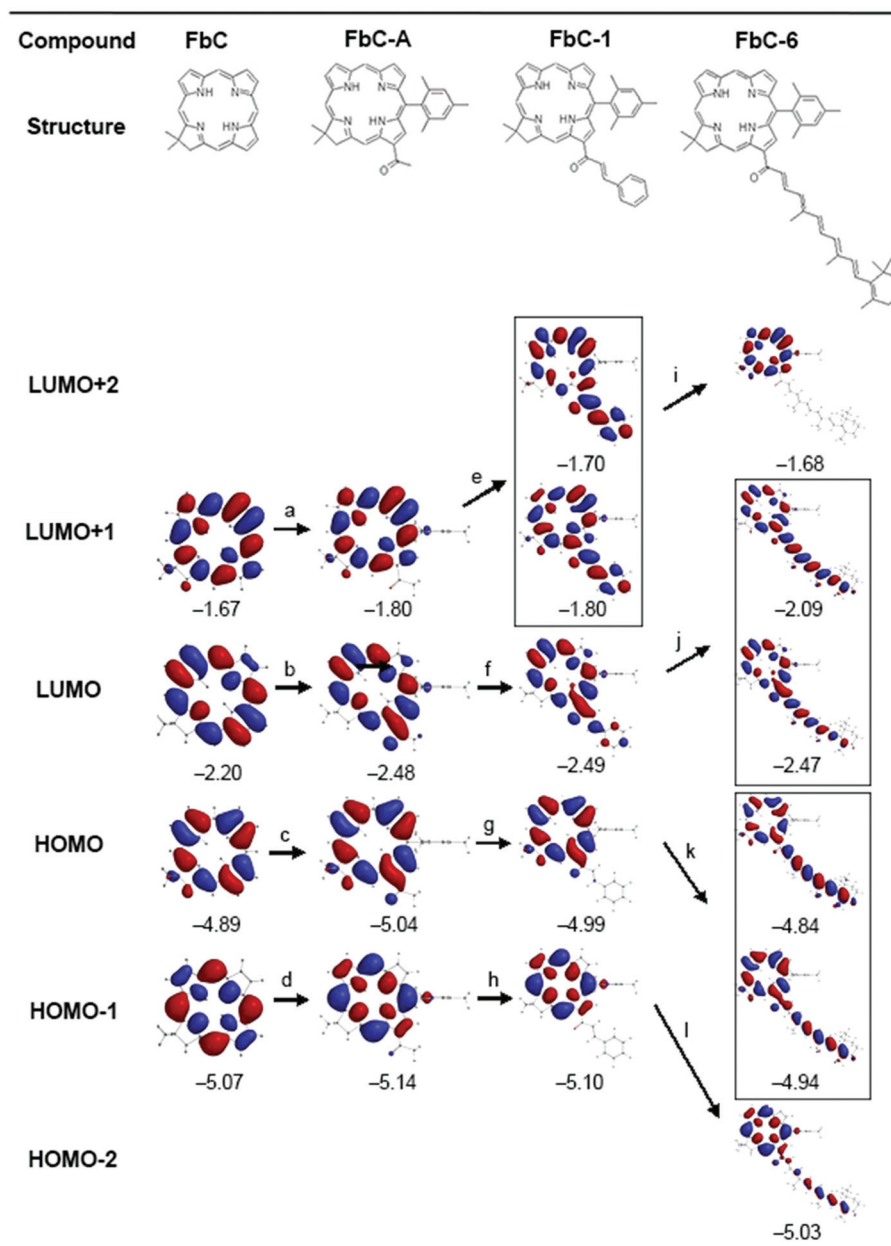


Fig. 10 Characteristics of the three lowest unoccupied and three highest occupied MOs of free base chlorins. The lettered arrows are as in Fig. 9.

the excited-state properties of the retinylidene–chalcone benchmark (I) with related compounds studied previously. We then turn to the chlorin systems. We first discuss the effects of the 13-substituent (acetyl, chalcone with one or six carbon-carbon double bond(s)) on the energies and electron-density distributions of the frontier MOs. A feature of this discussion is how interactions between substituent and chlorin macrocycle are manifested in the nature and number of orbitals in the normal HOMO–1 to LUMO+1 energy regime. We then examine the relationship of the MO properties to the absorption spectra, followed by a description of the relationship to the photophysical properties and an outlook for the utility of the new architectures.

Molecular design

One of the challenges in artificial photosynthesis is to identify rapid routes for the preparation of molecular architectures for solar light-harvesting and energy conversion. The retinylidene–chlorin–chalcone is an example of two commonplace chromophores joined *via* a readily constructed linker. The joining reaction that creates the chalcone linker makes use of all-*trans*-retinal and a synthetic acetylchlorin. Advances in chlorin synthetic chemistry have now made available a wide variety of chlorins either by *de novo* synthesis or by semisynthesis from porphyrins or chlorophylls.^{28–30} The acetylchlorin employed herein contains a geminal dimethyl group in the reduced

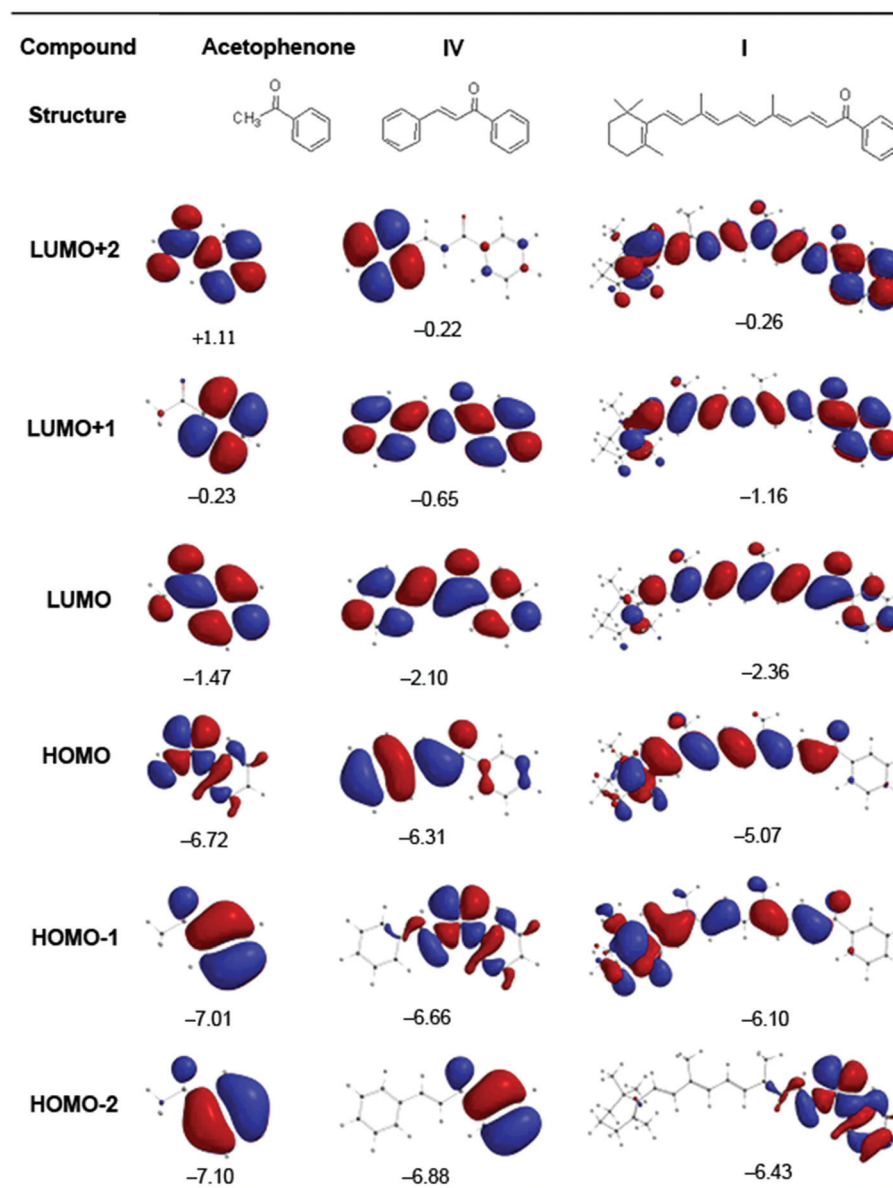


Fig. 11 Characteristics of the three lowest unoccupied and three highest occupied MOs of benchmarks acetophenone (for ZnC-A and FbC-A), IV (for ZnC-1 and FbC-1), and I (for ZnC-6 and FbC-6).

(pyrroline) ring, a feature that precludes adventitious dehydrogenation leading to the porphyrin. The acetyl group is located at the 13-position, which is the location of the keto group of the isocyclic ring of chlorophylls and also lies along the axis coincident with the transition that gives rise to the long-wavelength (Q_y) absorption band. All-*trans*-retinal, of course, is derived by oxidative homolysis of β -carotene. A wide variety of retinals are readily available *via* synthesis given the extensive studies of rhodopsins and bacteriorhodopsins.³¹ Nonetheless, surprisingly few retinylidene-chalcones have been prepared^{21,22} despite the facile methods for synthesis.^{10,11} Examples include **II** and **III** in Chart 2.

To our knowledge, the only other examples of tetrapyrrole-chalcones include several bacteriochlorin-chalcones⁸ and

a handful of *meso*-tetraarylporphyrins bearing appended chalcones.³² The retinylidene-chalcone moiety has some structural resemblance with carotenoids. In this regard, numerous carotenoid-tetrapyrrole constructs have been prepared in pioneering and comprehensive work by the team of Gust, Moore, and Moore (for reviews, see ref. 33–35; for selected reports, see ref. 36–39).^{33–39} Such constructs have been examined for light-harvesting and photoprotection properties that resemble those of the natural systems.⁴⁰ The carotenoids in such dyads and larger architectures generally contain 8–11 double bonds in the polyene chain, which is substantially longer than the 6 double bonds of the retinylidene-chalcone moiety examined herein.

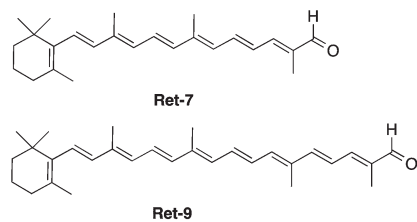


Chart 3 Homologues of all-*trans*-retinal (Ret-5).

Excited-state dynamics of retinylidene benchmark I

Native carotenoids such as peridinin and fucoxanthin and synthetic analogues bearing one or more carbonyl groups have been studied extensively using time-resolved absorption spectroscopy.^{41–48} A typical (but not universal) characteristic of these systems is the role of an intramolecular charge transfer (ICT) state involving the carbonyl moiety. Multi-exponential decays are ascribed to internal conversions involving the S_2 , S_1 , and ICT excited states and the S_0 ground state. Solvent dependence of the dynamics typically decreases as the length of the π -system increases. The solvent effects are ascribed to stabilization of the ICT state and thus, its energy relative to the S_1 and S_0 states.

One such example is the compound denoted **Ret-7** in Chart 3 for which decay of the ICT state (or mixed ICT/ S_1 state) to S_0 decreases from ~ 200 ps (in *n*-hexane or toluene) to ~ 20 ps (in acetone or ethanol) to ~ 7 ps (in methanol).⁴⁵ Increasing the chain length by two double bonds in analogue **Ret-9** reduces the solvent effect such that the time constant changes from ~ 25 ps (in isooctane or toluene) to ~ 15 ps (in acetone or ethanol) to ~ 8 ps (in methanol).⁴⁵ Another example is the retinylidene analogue **III** (Chart 2), which is similar to **I** except for the presence of the second carbonyl group.⁴⁸ Excited-state decay to S_0 takes ~ 6 ps in *n*-hexane, ~ 11 ps in toluene or acetone, and ~ 14 ps in methanol. The results and theoretical studies of **III** suggested that the dynamics do not involve an ICT state but may involve an (n,π^*) excited state, at least in one excited-state population.

The lifetimes observed herein for return of **I** to the ground state of 6.5 ps and 60 ps (1 : 1 ratio) in toluene and 15 ps in DMSO are in the range found for the above-noted related compounds and others.^{39,41–46,48} A change from 60 ps (at least in one excited-state population) in toluene to 15 ps in DMSO and companion changes in the shape of the transient absorption spectrum (Fig. 8) could suggest an enhanced contribution of an ICT state. Nevertheless, what is most germane herein is that the retinyl-like excited states responsible for the rapid (tens of picoseconds) decay of **I** to the ground state are not involved in the decay of the chlorin Q_y excited state of **ZnC-6** or **FbC-6** in toluene, where multi-nanosecond S_1 lifetimes are observed (Table 3). It seems clear that some type of CT underlies the short (~ 15 ps) excited-state decay for **ZnC-6** in DMSO and the ~ 1 ns component for **FbC-6** in this solvent. We will return to the nature of such states once a MO framework has been established in the following.

Molecular-orbital characteristics

The energies of all four standard chlorin frontier MOs (HOMO–1, HOMO, LUMO, LUMO+1) are altered (typically stabilized) by auxochromes such as the 13-acetyl group of **ZnC-A** and **FbC-A** relative to analogues that lack such groups such as **ZnC** and **FbC**; the 10-mesityl group has small effects by comparison.^{3,4} The LUMO is preferentially stabilized relative to the HOMO, LUMO+1 and LUMO–1 (Fig. 9 and 10). Significantly more (yet modest) electron density is observed on the acetyl oxygen in the LUMO and HOMO than in the LUMO+1 and HOMO–1. Such effects are designated by the arrows lettered ‘a’–‘d’ in Fig. 9 and 10.

Switching from the 13-acetyl group of **ZnC-A** and **FbC-A** to the short (one carbon–carbon double bond) 13-chalcone group of **ZnC-1** and **FbC-1** results in only small (≤ 0.05 eV) differences in the HOMO–1, HOMO, and LUMO energies, and the electron distribution on the macrocycle is essentially unchanged (arrows lettered ‘f’–‘h’ in Fig. 9 and 10). The electron density on the substituent oxygen is comparable for chalcone *versus* acetyl (along with density on the chalcone phenyl ring) for the LUMO, less on chalcone *versus* acetyl for the HOMO, and is minor on the chalcone enone moiety for the HOMO–1.

A major difference upon switching the 13-substituent from acetyl to the short chalcone is splitting of the normal chlorin LUMO+1 into the LUMO+1/LUMO+2 pair of orbitals, as indicated in the box preceded by arrow ‘e’ in Fig. 9 for **ZnC-1** and Fig. 10 for **FbC-1**. As can be seen from the figures and Table 4, the two orbitals of the LUMO+1/LUMO+2 pair are split by only 0.04 eV for **ZnC-1** and by 0.10 eV for **FbC-1**, with small (0–0.1 eV) individual shifts from the LUMO+1 of **ZnC-A** and **FbC-A**. Both orbitals of the LUMO+1/LUMO+2 pair have substantial electron density on both the short chalcone substituent and the macrocycle, but with different relative magnitudes for **ZnC-1** and **FbC-1**.

These combined considerations suggest that electron promotion from HOMO–1 or HOMO to a member of the LUMO+1/LUMO+2 pair for **ZnC-1** or **FbC-1** produces an excited-state configuration in the same energy regime as for electron promotion from HOMO–1 or HOMO to LUMO+1 for the benchmarks (**ZnC-A**, **FbC-A**, **ZnC**, **FbC**) but having substantially more chlorin \rightarrow chalcone CT character. This character may differ for **ZnC-1** and **FbC-1** depending on the relative contributions of the orbitals in the LUMO+1/LUMO+2 pair. Potential impacts on the absorption spectra and excited-state properties are discussed below.

Related observations, but with significant differences in detail, can be made for a switch of the 13-substituent from acetyl to the long chalcone group (six carbon–carbon double bonds) of **ZnC-6** and **FbC-6**. Tracing arrows ‘c’, ‘g’ and ‘k’ in Fig. 9 and 10 shows that for both **ZnC-6** and **FbC-6** the chlorin HOMO is split into a HOMO–1/HOMO pair, spaced by ~ 0.1 eV. Similarly, tracing arrows ‘b’, ‘f’ and ‘j’ in Fig. 9 and 10 shows that for both **ZnC-6** and **FbC-6** the chlorin LUMO is split into a LUMO/LUMO+1 pair, spaced by 0.36–0.38 eV. Both

Table 4 Molecular-orbital energies of chlorins^a

	HOMO-1	HOMO	LUMO	LUMO+1	LUMO-HOMO
ZnC	-5.10	-4.79	-2.12	-1.55	2.67
ZnC-A	-5.23	-4.95	-2.42	-1.68	2.53
ZnC-1	-5.19	-4.91	-2.43	[-1.68, -1.64]	2.48
ZnC-6	-5.12	[-4.88, -4.79]	[-2.41, -2.05]	-1.57	2.61 ^b
FbC	-5.07	-4.89	-2.20	-1.67	2.69
FbC-A	-5.14	-5.04	-2.48	-1.80	2.56
FbC-1	-5.10	-4.99	-2.49	[-1.80, -1.70]	2.50
FbC-6	-5.03	[-4.98, -4.84]	[-2.47, -2.09]	-1.68	2.63 ^b
Acetophenone	-7.01	-6.72	-1.47	-0.23	5.25
IV	-6.66	-6.31	-2.10	-0.65	4.21
I	-6.10	-5.07	-2.36	-1.16	2.71

^a From DFT calculations. Entries in columns 2-4 for the chlorin-chalcones (ZnC-1, FbC-1, ZnC-6, FbC-6) are the individual orbitals or pairs of orbitals (in square brackets) that have electron-density distributions on the macrocycle that are the closest to the "normal" frontier MOs (*e.g.*, those for ZnC or FbC), as can be seen from Fig. 9 and 10. For example, because the listed 'HOMO' of ZnC-6 is a pair of orbitals (the actual HOMO and HOMO-1) the listed 'HOMO-1' is the HOMO-2 for this molecule (Fig. 9). ^b For ZnC-6 and FbC-6, the energies of the two orbitals listed as the 'HOMO' are averaged and the energies of the two orbitals listed as the 'LUMO' are averaged in calculating the LUMO-HOMO gap.

members of the HOMO-1/HOMO pair and both members of the LUMO/LUMO+1 pair have substantial electron density spread along the length of the long 13-chalcone substituent of ZnC-6 and FbC-6.

As a result of the splitting of the HOMO into the HOMO-1/HOMO pair and the LUMO into the LUMO/LUMO+1 pair, the benchmark chlorin HOMO-1 becomes the HOMO-2 (arrows 'd', 'h' and 'l'), and the chlorin LUMO+1 becomes the LUMO+2 (arrows 'a', 'e' and 'i') for ZnC-6 and FbC-6. For these two chlorins, the energy shifts of the HOMO-2 and LUMO+2 from the respective HOMO-1 and LUMO+1 of ZnC-A and FbC-A is roughly 0.1 eV. The LUMO+2 of ZnC-6 and FbC-6 has essentially no electron density on the retinylidene unit; hence, electron promotion to this orbital from a member of the HOMO-1/HOMO pair gives an excited-state configuration with substantial CT character. Additionally, differences in the electron-density on the long chalcone (retinylidene) group in the HOMO-2 for ZnC-6 versus FbC-6 and with the unoccupied MOs suggests that electron promotions involving these orbitals will produce configurations with varying degrees of CT character.

The splitting of the benchmark chlorin HOMO into a HOMO/HOMO-1 for ZnC-6 must arise in part because the HOMO energy of I (-5.07 eV; Fig. 11) is comparable to that of the simple chlorins (-4.95 eV, ZnC-A), thereby facilitating chlorin-chalcone MO mixing. The same phenomenon is true for FbC-6. On the other hand, the HOMO energy for the shorter (one carbon-carbon double bond) chalcone benchmark IV (-6.31 eV) or the acetyl benchmark acetophenone (-6.72 eV) are substantially lower than the typical chlorin HOMO (for ZnC-A, FbC-A, ZnC, FbC) giving rise to less orbital mixing. Similar arguments apply for the generation of a LUMO/LUMO+1 pair for ZnC-6 and FbC-6. In particular, the LUMO energy of I (-2.36 eV) is comparable to that of the chlorins (-2.42 eV, ZnC-A). Additionally, comparison of these values and the similar LUMO energy of benchmark IV (-2.10 eV) may underlie why the LUMO of ZnC-1 and FbC-1 has appreciable electron density on the short chalcone group (Fig. 9 and 10).

Potential relationships of such differences in MO characteristics with photophysical properties of the chlorins are given below.

Optical properties

In a simple one-electron model, a trend in the LUMO-HOMO energy gap often correlates with the relative energies (and absorption wavelengths) of the lowest singlet excited state (S_1). The data in Fig. 11 and Table 4 indicate that the LUMO-HOMO gap decreases as the conjugation length of the benchmark (and corresponding 13-substituent of the chlorin) increases along the series I (2.71 eV; long chalcone) < IV (4.21 eV; short chalcone) < acetophenone (5.25 eV; acetyl). The substantially lower LUMO-HOMO gap for I no doubt underlies the shift of the long-wavelength transition into the visible region (Fig. 1).

The LUMO-HOMO gap for I (2.71 eV) is comparable to the typical LUMO-HOMO gap of chlorins (~2.5 eV; Table 4). The Q_y energy for each chlorin is considerably lower than indicated by the LUMO-HOMO gap because the simple one-electron (particle-in-a-circular-box) model is not sufficient. The complexity is revealed in Gouterman's four orbital model,⁴⁹⁻⁵¹ in which the Q_y and B_y excited states (and absorption bands) derive from linear combinations of the HOMO → LUMO and HOMO-1 → LUMO+1 configurations. The Q_y is roughly a 70/30 admixture of the two configurations and *vice versa* for B_y .⁵²⁻⁵⁵ Similarly, B_x and Q_x derive from the configurations resulting from one-electron promotions from HOMO to LUMO+1 and HOMO-1 to LUMO.

Inspection of Fig. 9 and 10 indicates that within the set of four zinc chlorins there is far less variation in the LUMO+1-HOMO-1 energy gap than in the LUMO-HOMO energy gap. The same is true of the four free base chlorins. Thus, although consideration of such mixing is essential to understand the actual energies and relative intensities of the bands, the trends in Q_y position are reasonably reflected in the trend in LUMO-HOMO energy gap. Such comparisons are relatively straightforward for understanding the bathochromic shift in

the Q_y upon the addition to **ZnC** (or **FbC**) of the 13-acetyl group to give **ZnC-A** (or **FbC-A**) and then switching to the short chalcone group to give **ZnC-1** (or **FbC-1**). The situation is more complex for **ZnC-6** and **FbC-6** because pairs of orbitals are derived from mixing of the chlorin HOMO and LUMO with orbitals of the long (retinylidene) chalcone group (*vide supra*). Nonetheless, the nominal Q_y and B_y bands (like the orbitals involved) are in the proper energy regime and retain substantial characteristics of the chlorin macrocycle.

Given the MO characteristics, it is not certain whether the new absorption in the 450–500 nm region of **ZnC-6** and **FbC-6** (relative to the benchmarks) is best described as having mixed chlorin–retinylidene parentage or reflecting transition(s) more localized on the long conjugated 13-substituent. Although the MO characteristics suggest the possibility that absorption in this region could involve excited states with some net macrocycle \leftrightarrow chalcone CT character, the dependence on solvent polarity is not substantially different than that for the other absorption features (Fig. 2 and 3). Regardless, the absorption in the 450–500 nm region of these chlorin–chalcones leads to quantitative formation of the Q_y excited state (*vide supra*). It is the decay properties of that state to which we now turn.

Excited-state properties

The description of the frontier MOs given above affords a foundation for understanding how, depending on compound and solvent polarity, excited-states with chlorin \leftrightarrow chalcone CT character could participate in photophysical properties such as the fluorescence quantum yields and excited-state lifetimes. For the unsubstituted chlorins (**ZnC** and **FbC**) and the acetyl chlorins (**ZnC-A** and **FbC-A**), there is essentially no electron density on the 13-substituent. Thus, all electron promotions from HOMO–1 or HOMO to LUMO or LUMO+1 will be entirely chlorin based. On the other hand, for the chlorin–chalcones, and most notably **ZnC-6** and **FbC-6**, a number of electron promotions involving the frontier MOs will produce an excited state with chlorin \leftrightarrow chalcone CT character. One example is electron promotion from a member of the HOMO–1/HOMO pair (derived from the chlorin HOMO) to LUMO+2 (basically the benchmark chlorin LUMO+1). Additionally, the greater electron density on the HOMO–2 for **FbC-6** will produce less CT character upon electron promotion to the LUMO or LUMO+1 relative to **ZnC-6**. The latter difference may contribute to the far less substantial reduction in Φ_f and τ_S for **FbC-6** compared to **ZnC-6** when the solvent is changed from toluene to DMSO. Also contributing to that difference in behavior are the relative redox properties of the zinc and free base chlorins,⁵⁶ as reflected in the relative HOMO (chlorin oxidation) and LUMO (chlorin reduction) energies (Fig. 9 and 10).

The rationale for ascribing reduced Φ_f and τ_S values for **FbC-6** and more so for **ZnC-6** in DMSO *versus* toluene (Table 3) to a state with chlorin \leftrightarrow chalcone CT character is that such states would be stabilized in the more polar solvent. Such a state could mix with the normal chlorin S_1 (Q_y) or drop to lower energy and act as a quencher. The consequence is an enhanced effective rate constant for internal conversion with

the simple trifurcation model for S_1 excited-state decay used to derive the rate constants (k_f , k_{isc} , k_{ic}) listed in Table 3.

The result for **FbC-6** in DMSO is that Φ_f is about half that for **FbC-1** in DMSO (0.13 *versus* 0.24) and τ_S has a short component (~ 1 ns) that is about 7-fold reduced from the longer component (~ 7.4 ns) for this compound (**FbC-6**) and that for **FbC-1** (7.3 ns) in this solvent. The quenching apparently occurs in one of two (or more) excited-state populations that likely result from different conformers associated with the retinylidene moiety and/or its disposition with respect to the chlorin macrocycle. The likely contribution of a state with chlorin \leftrightarrow chalcone CT character for **ZnC-6** in DMSO results in complete excited-state decay to the ground state with a time constant of ~ 15 ps. This lifetime could reflect the decay of the CT-like state and not the nominal S_1 state from which it is borne, which would have a shorter lifetime still.

Outlook

The ability to design molecular architectures with desired spectral properties is of fundamental importance in artificial photosynthesis. Systematic tuning of spectral properties (wavelength, intensity) of a given tetrapyrrole macrocycle (porphyrin, chlorin, bacteriochlorin) in modest increments across rather large spectral regions can be attained through the use of simple auxochromes (*e.g.*, phenyl, vinyl, ethynyl, acetyl, formyl). However, such tuning is generally achieved by the effects of the substituents on the energies of the tetrapyrrole MOs and excited-state electronic configurations and a redistribution of the oscillator strength within the tetrapyrrole excited-state manifold. An approach to achieve more extensive spectral coverage is to tightly couple to the tetrapyrrole more potent, highly conjugated substituents that bring new absorption into a target spectral region. Herein, the chlorin–chalcones have been found to exhibit strongly bathochromically shifted (and intense) Q_y absorption bands and long excited-state lifetimes. The long lifetimes and bright fluorescence are accompanied by enhanced absorption in the 400–500 nm region for retinylidene-containing **FbC-6** and **ZnC-6** where chlorins alone – or chlorins bearing simple auxochromes – have little or no oscillator strength. The enhanced absorption in the 400–500 nm region gives rise to quantitative formation of the chlorin Q_y excited state, thereby affording enhanced solar coverage.

Experimental methods

Photophysical studies

Fluorescence yields, singlet excited-state lifetimes, and intersystem-crossing (triplet) yields were measured as described previously.^{4,6} In short, fluorescence lifetimes are typically the average from measurements (Soret excitation) using a phase-modulation technique and a time-resolved instrument with a ~ 1 ns response function. Transient absorption studies typically utilized ~ 100 fs excitation pulses (in the Soret, Q_x or Q_y bands) with an energy of 0.5 μ J and a diameter of 1 mm. The standard

for fluorescence quantum yields was chlorophyll *a* in deoxygenated toluene ($\Phi_f = 0.325$),²⁵ which is the value in deoxygenated benzene.²⁶ Samples used for static absorption and fluorescence studies typically had a chlorin concentration of 0.2–0.7 μM in a 1 cm path cuvette ($A \leq 0.1$ at the excitation wavelength) and those for transient absorption studies were about 3-fold more concentrated in a 2 mm path cell.

Molecular-orbital calculations

DFT calculations were performed with Spartan '10 for Windows version 1.2.0 using the hybrid B3LYP functional, 6-31G* basis set, and equilibrium geometries optimized using the default parameters.⁵⁷ Molecular-orbital (MO) images were plotted from Spartan using an isovalue of 0.016.

Acknowledgements

This work was supported by grants from the Division of Chemical Sciences, Geosciences, and Biosciences, Office of Basic Energy Sciences of the U.S. Department of Energy to D.F.B. (DE-FG02-05ER15660), D.H. (DE-FG02-05ER15661) and J.S.L. (DE-FG02-96ER14632). Mass spectra were obtained at the Mass Spectrometry Laboratory for Biotechnology at North Carolina State University. Partial funding for the facility was obtained from the North Carolina Biotechnology Center and the National Science Foundation. Transient absorption studies were performed in the Ultrafast Laser Facility of the Photosynthetic Antenna Research Center (PARC), an Energy Frontier Research Center funded by the U.S. Department of Energy, Office of Science, Office of Basic Energy Sciences, under Award No. DE-SC0001035.

References

- H. Scheer, An overview of chlorophylls and bacteriochlorophylls: Biochemistry, biophysics, functions and applications, in *Chlorophylls and Bacteriochlorophylls. Biochemistry, Biophysics, Functions and Applications*, ed. B. Grimm, R. J. Porra, W. Rüdiger and H. Scheer, Springer, Dordrecht, The Netherlands, 2006, vol. 25, pp. 1–26.
- H. L. Kee, C. Kirmaier, Q. Tang, J. R. Diers, C. Muthiah, M. Taniguchi, J. K. Laha, M. Ptaszek, J. S. Lindsey, D. F. Bocian and D. Holten, Effects of substituents on synthetic analogs of chlorophylls. Part 1: Synthesis, vibrational properties and excited-state decay characteristics, *Photochem. Photobiol.*, 2007, **83**, 1110–1124.
- H. L. Kee, C. Kirmaier, Q. Tang, J. R. Diers, C. Muthiah, M. Taniguchi, J. K. Laha, M. Ptaszek, J. S. Lindsey, D. F. Bocian and D. Holten, Effects of substituents on synthetic analogs of chlorophylls. Part 2: Redox properties, optical spectra and electronic structure, *Photochem. Photobiol.*, 2007, **83**, 1125–1143.
- J. W. Springer, K. M. Faries, H. L. Kee, J. R. Diers, C. Muthiah, O. Mass, C. Kirmaier, J. S. Lindsey, D. F. Bocian and D. Holten, Effects of substituents on synthetic analogs of chlorophylls. Part 3: The distinctive impact of auxochromes at the 7- versus 3-positions, *Photochem. Photobiol.*, 2012, **88**, 651–674.
- M. Taniguchi, D. L. Cramer, A. D. Bhise, H. L. Kee, D. F. Bocian, D. Holten and J. S. Lindsey, Accessing the near-infrared spectral region with stable, synthetic, wavelength-tunable bacteriochlorins, *New J. Chem.*, 2008, **32**, 947–958.
- E. Yang, C. Kirmaier, M. Krayer, M. Taniguchi, H.-J. Kim, J. R. Diers, D. F. Bocian, J. S. Lindsey and D. Holten, Photo-physical properties and electronic structure of stable, tunable synthetic bacteriochlorins: Extending the features of native photosynthetic pigments, *J. Phys. Chem. B*, 2011, **115**, 10801–10816.
- C.-Y. Chen, E. Sun, D. Fan, M. Taniguchi, B. E. McDowell, E. Yang, J. R. Diers, D. F. Bocian, D. Holten and J. S. Lindsey, Synthesis and physicochemical properties of metallo-bacteriochlorins, *Inorg. Chem.*, 2012, **51**, 9443–9464.
- E. Yang, C. Ruzié, M. Krayer, J. R. Diers, D. M. Niedzwiedzki, C. Kirmaier, J. S. Lindsey, D. F. Bocian and D. Holten, Photophysical properties and electronic structure of bacteriochlorin–chalcones with extended near-infrared absorption, *Photochem. Photobiol.*, 2013, **89**, 586–604.
- S. V. Kostanecki and J. Tambor, Ueber die sechs isomeren monoxybenzalacetophenone (monoxychalkone), *Chem. Ber.*, 1899, **32**, 1921–1926.
- D. N. Dhar, *The Chemistry of Chalcones and Related Compounds*, John Wiley & Sons, Inc., New York, 1981.
- S. N. A. Bukhari, M. Jasamai and I. Jantan, Synthesis and biological evaluation of chalcone derivatives (mini review), *Mini-Rev. Med. Chem.*, 2012, **12**, 1394–1403.
- R. E. Koes, F. Quattrocchio and J. N. M. Mol, The flavonoid biosynthetic pathway in plants: function and evolution, *Bioessays*, 1994, **16**, 123–132.
- K. Springob, J.-I. Nakajima, M. Yamazaki and K. Saito, Recent advances in the biosynthesis and accumulation of anthocyanins, *Nat. Prod. Rep.*, 2003, **20**, 288–303.
- M. B. Austin and J. P. Noel, The chalcone synthase superfamily of type III polyketide synthases, *Nat. Prod. Rep.*, 2003, **20**, 79–110.
- E. Grotewold, The genetics and biochemistry of floral pigments, *Annu. Rev. Plant Biol.*, 2006, **57**, 761–780.
- C. Ruzié, M. Krayer and J. S. Lindsey, Fast and robust route to hydroporphyrin–chalcones with extended red or near-infrared absorption, *Org. Lett.*, 2009, **11**, 1761–1764.
- K. Aravindu, H.-J. Kim, M. Taniguchi, P. L. Dilbeck, J. R. Diers, D. F. Bocian, D. Holten and J. S. Lindsey, Synthesis and photophysical properties of chlorins bearing 0–4 distinct meso-substituents, *Photochem. Photobiol. Sci.*, 2013, **12**, 2089–2109.
- J. K. Laha, C. Muthiah, M. Taniguchi, B. E. McDowell, M. Ptaszek and J. S. Lindsey, Synthetic chlorins bearing

- auxochromes at the 3- and 13-positions, *J. Org. Chem.*, 2006, **71**, 4092–4102. Erratum: *J. Org. Chem.*, 2009, **74**, 5122.
- 19 M. Taniguchi, M. Ptaszek, B. E. McDowell and J. S. Lindsey, Sparsely substituted chlorins as core constructs in chlorophyll analogue chemistry. Part 2: Derivatization, *Tetrahedron*, 2007, **63**, 3840–3849.
- 20 C.-B. An, R. Liang, X.-H. Ma, L.-M. Fu, J.-P. Zhang, P. Wang, R.-M. Han, X.-C. Ai and L. H. Skibsted, Retinylisoflavonoid as a novel membrane antioxidant, *J. Phys. Chem. B*, 2010, **114**, 13904–13910.
- 21 H. Hashimoto, K. Hattori, Y. Okada, T. Yoda and R. Matsushima, Molecular and crystal structures of 2-(all-trans-retinylidene)-indan-1,3-dione, *Jpn. J. Appl. Phys.*, 1998, **37**, 4609–4615.
- 22 N. Acton, A. Brossi, D. L. Newton and M. B. Sporn, Potential prophylactic antitumor activity of retinylidene 1,3-diketones, *J. Med. Chem.*, 1980, **23**, 805–809.
- 23 K.-W. Wang, S.-W. Wang and Q.-Z. Du, Complete NMR assignment of retinal and its related compounds, *Magn. Reson. Chem.*, 2013, **51**, 435–438.
- 24 S. J. Lee, K. C. Gray, J. S. Paek and M. D. Burke, Simple, efficient, and modular syntheses of polyene natural products via iterative cross-coupling, *J. Am. Chem. Soc.*, 2008, **130**, 466–468.
- 25 O. Mass, M. Taniguchi, M. Ptaszek, J. W. Springer, K. M. Faries, J. R. Diers, D. F. Bocian, D. Holten and J. S. Lindsey, Structural characteristics that make chlorophylls green: interplay of hydrocarbon skeleton and substituents, *New J. Chem.*, 2011, **35**, 76–88.
- 26 G. Weber and F. W. J. Teale, Determination of the absolute quantum yield of fluorescent solutions, *Trans. Faraday Soc.*, 1957, **53**, 646–655.
- 27 J. B. Birks, *Photophysics of Aromatic Molecules*, Wiley-Interscience, London, 1970, pp. 142–192.
- 28 F.-P. Montforts, B. Gerlach and F. Höper, Discovery and synthesis of less common natural hydroporphyrins, *Chem. Rev.*, 1994, **94**, 327–347.
- 29 V. Y. Pavlov and G. V. Ponomarev, Modification of the peripheral substituents in chlorophylls *a* and *b* and their derivatives (review), *Chem. Heterocycl. Compd.*, 2004, **40**, 393–425.
- 30 M. Galezowski and D. T. Gryko, Recent advances in the synthesis of hydroporphyrins, *Curr. Org. Chem.*, 2007, **11**, 1310–1338.
- 31 A. K. Singh and P. K. Hota, Development of bacteriorhodopsin analogues and studies of charge separated excited states in the photoprocesses of linear polyenes, *Photochem. Photobiol.*, 2007, **83**, 50–62.
- 32 V. Vaz Serra, F. Camões, S. I. Vieira, M. A. F. Faustino, J. P. C. Tomé, D. C. G. A. Pinto, M. G. P. M. S. Neves, A. C. Tomé, A. M. S. Silva, E. F. da Cruz e Silva and J. A. S. Cavaleiro, Synthesis and biological evaluation of novel chalcone-porphyrin conjugates, *Acta Chim. Slov.*, 2009, **56**, 603–611.
- 33 D. Gust, T. A. Moore and A. L. Moore, Molecular mimicry of photosynthetic energy and electron transfer, *Acc. Chem. Res.*, 1993, **26**, 198–205.
- 34 D. Gust, T. A. Moore and A. L. Moore, Mimicking photosynthetic solar energy transduction, *Acc. Chem. Res.*, 2001, **34**, 40–48.
- 35 T. A. Moore, A. L. Moore and D. Gust, The design and synthesis of artificial photosynthetic antennas, reaction centres and membranes, *Philos. Trans. R. Soc. London, Ser. B*, 2002, **357**, 1481–1498.
- 36 F. Fungo, L. Otero, E. N. Durantini, J. J. Silber, L. Sereno, E. Mariño-Ochoa, T. A. Moore, A. L. Moore and D. Gust, Photoelectrochemistry of a pigment used in artificial photosynthesis: an anilino-carotenoid, *J. Phys. Chem. B*, 2001, **105**, 4783–4790.
- 37 S. L. Gould, G. Kodis, P. A. Liddell, R. E. Palacios, A. Brune, D. Gust, T. A. Moore and A. L. Moore, Artificial photosynthetic reaction centers with carotenoid antennas, *Tetrahedron*, 2006, **62**, 2074–2096.
- 38 M. Kloz, S. Pillai, G. Kodis, D. Gust, T. A. Moore, A. L. Moore, R. van Grondelle and J. T. M. Kennis, Carotenoid photoprotection in artificial photosynthetic antennas, *J. Am. Chem. Soc.*, 2011, **133**, 7007–7015.
- 39 M. Kloz, S. Pillai, G. Kodis, D. Gust, T. A. Moore, A. L. Moore, R. van Grondelle and J. T. M. Kennis, New light-harvesting roles of hot and forbidden carotenoid states in artificial photosynthetic constructs, *Chem. Sci.*, 2012, **3**, 2052–2061.
- 40 T. Polívka and H. A. Frank, Molecular factors controlling photosynthetic light harvesting by carotenoids, *Acc. Chem. Res.*, 2010, **43**, 1125–1134.
- 41 J. A. Bautista, R. E. Connors, B. B. Raju, R. G. Hiller, F. P. Sharples, D. Gosztola, M. R. Wasielewski and H. A. Frank, Excited state properties of peridinin: Observation of a solvent dependence of the lowest excited singlet state lifetime and spectral behavior unique among carotenoids, *J. Phys. Chem. B*, 1999, **103**, 8751–8758.
- 42 H. A. Frank, J. A. Bautista, J. Josue, Z. Pendon, R. G. Hiller, F. P. Sharples, D. Gosztola and M. R. Wasielewski, Effect of the solvent environment on the spectroscopic properties and dynamics of the lowest excited states of carotenoids, *J. Phys. Chem. B*, 2000, **104**, 4569–4577.
- 43 D. A. Wild, K. Winkler, S. Stalke, K. Oum and T. Lenzer, Extremely strong solvent dependence of the $S_1 \rightarrow S_0$ internal conversion lifetime of 12'-apo- β -caroten-12'-al, *Phys. Chem. Chem. Phys.*, 2006, **8**, 2499–2505.
- 44 F. Ehlers, D. A. Wild, T. Lenzer and K. Oum, Investigation of the $S_1/ICT \rightarrow S_0$ internal conversion lifetime of 4'-apo- β -caroten-4'-al and 8'-apo- β -caroten-8'-al: Dependence on conjugation length and solvent polarity, *J. Phys. Chem. A*, 2007, **111**, 2257–2265.
- 45 M. Kopczynski, F. Ehlers, T. Lenzer and K. Oum, Evidence for an intramolecular charge transfer state in 12'-apo- β -caroten-12'-al and 8'-apo- β -caroten-8'-al: Influence of solvent polarity and temperature, *J. Phys. Chem. A*, 2007, **111**, 5370–5381.

- 46 D. M. Niedzwiedzki, N. Chatterjee, M. M. Enriquez, T. Kajikawa, S. Hasegawa, S. Katsumura and H. A. Frank, Spectroscopic investigation of peridinin analogues having different π -electron conjugated chain lengths: Exploring the nature of the intramolecular charge transfer state, *J. Phys. Chem. B*, 2009, **113**, 13604–13612.
- 47 T. Polívka and H. A. Frank, Molecular factors controlling photosynthetic light harvesting by carotenoids, *Acc. Chem. Res.*, 2010, **43**, 1125–1134.
- 48 T. Kusumoto, D. Kosumi, C. Uragami, H. A. Frank, R. R. Birge, R. J. Cogdell and H. Hashimoto, Femtosecond transient absorption spectroscopic study of a carbonyl-containing carotenoid analogue, 2-(all-*trans*-retinylidene)-indan-1,3-dione, *J. Phys. Chem. A*, 2011, **115**, 2110–2119.
- 49 M. Gouterman, Study of the effects of substitution on the absorption spectra of porphin, *J. Chem. Phys.*, 1959, **30**, 1139–1161.
- 50 M. Gouterman, Spectra of porphyrins, *J. Mol. Spectrosc.*, 1961, **6**, 138–163.
- 51 M. Gouterman, Optical spectra and electronic structure of porphyrins and related rings, in *The Porphyrins*, ed. D. Dolphin, Academic Press, New York, 1978, vol. 3, pp. 1–165.
- 52 C. Weiss Jr., The pi electron structure and absorption spectra of chlorophylls in solution, *J. Mol. Spectrosc.*, 1972, **44**, 37–80.
- 53 J. D. Petke, G. M. Maggiora, L. L. Shipman and R. E. Christoffersen, Stereoelectronic properties of photosynthetic and related systems. *Ab initio* configuration interaction calculations on the ground and lower excited singlet and triplet states of magnesium chlorin and chlorin, *J. Mol. Spectrosc.*, 1978, **73**, 311–331.
- 54 J. Linnanto and J. Korppi-Tommola, Quantum chemical simulation of excited states of chlorophylls, bacteriochlorophylls and their complexes, *Phys. Chem. Chem. Phys.*, 2006, **8**, 663–687.
- 55 L. Petit, A. Quartarolo, C. Adamo and N. Russo, Spectroscopic properties of porphyrin-like photosensitizers: Insights from theory, *J. Phys. Chem. B*, 2006, **110**, 2398–2404.
- 56 R. H. Felton, Primary redox reactions of metalloporphyrins, in *The Porphyrins*, ed. D. Dolphin, Academic Press, New York, 1978, vol. V, pp. 53–125.
- 57 Except for molecular mechanics and semi-empirical models, the calculation methods used in Spartan '08 or '10 have been documented in: Y. Shao, L. F. Molnar, Y. Jung, J. Kussmann, C. Ochsenfeld, S. T. Brown, A. T. B. Gilbert, L. V. Slipchenko, S. V. Levchenko, D. P. O'Neill, R. A. DiStasio Jr., R. C. Lochan, T. Wang, G. J. O. Beran, N. A. Besley, J. M. Herbert, C. Y. Lin, T. Van Voorhis, S. H. Chien, A. Sodt, R. P. Steele, V. A. Rassolov, P. E. Maslen, P. P. Korambath, R. D. Adamson, B. Austin, J. Baker, E. F. C. Byrd, H. Dachsel, R. J. Doerksen, A. Dreuw, B. D. Dunietz, A. D. Dutoi, T. R. Furlani, S. R. Gwaltney, A. Heyden, S. Hirata, C.-P. Hsu, G. Kedziora, R. Z. Khallulin, P. Klunzinger, A. M. Lee, M. S. Lee, W. Liang, I. Lotan, N. Nair, B. Peters, E. I. Proynov, P. A. Pieniazek, Y. M. Rhee, J. Ritchie, E. Rosta, C. D. Sherrill, A. C. Simmonett, J. E. Subotnik, H. L. Woodcock III, W. Zhang, A. T. Bell, A. K. Chakraborty, D. M. Chipman, F. J. Keil, A. Warshel, W. J. Hehre, H. F. Schaefer III, J. Kong, A. I. Krylov, P. M. W. Gill and M. Head-Gordon, Advances in methods and algorithms in a modern quantum chemistry program package, *Phys. Chem. Chem. Phys.*, 2006, **8**, 3172–3191.